Applied Catalysis B: Environmental 243 (2019) 161–174

Contents lists available at ScienceDirect

Applied Catalysis B: Environmental

journal homepage: www.elsevier.com/locate/apcatb

Iron-coated polymer films with high antibacterial activity under indoor and outdoor light, prepared by different facile pre-treatment and deposition methods

Laura Victoria Suárez Murillo, Ania Schärer, Stefanos Giannakis*, Sami Rtimi, César Pulgarín**

School of Basic Sciences (SB), Institute of Chemical Science and Engineering (ISIC), Group of Advanced Oxidation Processes (GPAO), École Polytechnique Fédérale de Lausanne (EPFL), Station 6, CH-1015, Lausanne, Switzerland

ARTICLE INFO

Keywords:
Antibacterial surfaces
Polymer films
Iron oxides
Solar disinfection and photo-fenton
Semiconductors

ABSTRACT

In the present work, we study the fabrication of self-cleaning antibacterial surfaces, active under indoor or outdoor light. In order to obtain the highest activity with the lowest complexity we assess mild conditions of preparation (temperatures), pre-treatment (physical, chemical) and deposition method (dip coating, spraying). We report that the combination of deposition time and temperature during this phase on PET can lead to effective germicidal films (< 40 min under solar light) and pre-treatment with simple sandpaper scratching or acetone dissolution increase the inactivation kinetics more than 35%. Spray coating always led to higher germicidal efficiencies, due to the differentiated layering during deposition, reaching total inactivation under either indoor or solar light. Furthermore, the non-pretreated films were very robust over 10 re-uses and the pre-treated ones led to virtually no loss of antibacterial activity. Other materials such as polyurethane (PU) and LDPE were effectively used, with pre-treated PU reaching the fastest inactivation (< 30 min). Finally, the costly Fe reagent was effectively replaced with natural Fe oxides, which were equally efficient in pre-treated surfaces. In overall, compared to real world conditions, a very high microbial load was eliminated, in either indoor or outdoor environments, meeting the demands where the infection problems are high and the means are scarce.

1. Introduction

Humans and microbes constantly interact, and among human microbiota most of the bacteria are harmless or even beneficial. However, around 30% of bacteria are pathogens. They can survive in surfaces and any contact with them leads to contamination by spreading, and evidence of this phenomenon was presented by Sanborn et al. [1]. This issue is particularly important in hospitals where hospital-acquired infections (HAIs) represent a health danger, especially combined with the increase of antibiotic resistance in bacteria [2,3]. A patient can be affected by HAIs after being in contact with contaminated medical utensils, but also after contact with frequently touched surfaces in hospitals. Rigorous sterilization of the medical equipment, appropriate hand washing and thorough cleaning are promoted to lower HAIs risk. Nonetheless, a study on methicillin-resistant *Staphylococcus aureus* (MRSA) contamination in hospitals found that MRSA is detected in 74% of cases prior to cleaning and on 66% of test surfaces after cleaning [4]. This is why the development of antibacterial films represents a way to address the problem, as a complement to proper hygiene and cleaning habits.

Development of appropriate self-disinfecting coatings, active under indoor and outdoor environments without any further intervention, could contribute to stop pathogens transmission. Several antimicrobial coatings have been developed; some are based on technologies as microbicide-releasing surfaces (e.g. Microban® [5]) or bacteriophage-modified surfaces [6]. However, bacteria may develop resistance to the released substances over time, and also, phages are specific to individual bacterial species. The light-activated antimicrobial coatings producing active species when illuminated are an alternative; the radicals (specially $^{\cdot}OH$) are non-specific and pathogens cannot develop resistance to them. TiO_2 semiconductor has been known to inactivate bacteria being dispersed in a solution or deposited as a coating; it gets activated by light generating electrons (e^-_{CB}) and holes (h^+_{VB}) that later on react with oxygen and/or water to produce the aforementioned radical species (reactive oxygen species, ROS). These species are hydroxyl ($^{\cdot}OH$), superoxide anion ($O_2^{\cdot-}$), hydroperoxyl ($^{\cdot}OOH$) radicals, and

* Corresponding author.
** Corresponding author.
E-mail addresses: Stefanos.Giannakis@epfl.ch (S. Giannakis), Cesar.Pulgarin@epfl.ch (C. Pulgarín).

https://doi.org/10.1016/j.apcatb.2018.10.035
Received 13 August 2018; Received in revised form 12 October 2018; Accepted 15 October 2018
Available online 16 October 2018
0926-3373/

hydrogen peroxide (H_2O_2) [7]; these ROS will attack the microorganisms by damaging the cell and subsequently modifying its components [8].

TiO_2 deposition has been addressed for preparing antibacterial films [9,10] by following various methods: sol-gel [11], sputtering [12,13], chemical vapor deposition [14], or dip-coating [15]. However, it has to be considered that the band-gap of TiO_2 is 3.2 eV which means it needs UVA-light photons with a wavelength under 385 nm to generate the electron/hole pair. This is a limitation that can be addressed by using semiconductors with narrower band-gap active under visible light, such as copper oxides or iron oxides. Copper oxides or copper doped TiO_2 have been studied for antibacterial approaches showing not only activity under light irradiation but also an oligodynamic effect on bacteria [16–18]. However, iron oxides can be advantageous for several reasons: a) they are less costly than copper oxides, b) they are highly available in nature, c) the human acceptance of iron in the organism is higher than for copper, avoiding risks for human health.

The semiconductor mode of action of iron oxides for bacterial inactivation also relies on a photon with energy equal or higher than the band gap to be absorbed to promote the electron/hole pair formation. The holes generated in most of the iron oxides have an oxidation potential of around 1.7–1.8 eV which is enough for attacking the bacterial cell wall but not for oxidizing water and generate $^{\cdot}OH$. There is however a production of $O_2^{\cdot -}$, which has a particular toxic effect on bacteria due to its affinity with the components of the bacterial cell wall. In former studies, goethite, hematite and wüstite were found to follow this mode of action [19], while similar outcomes were found on virus inactivation [20,21].

Iron oxide fixation onto substrates is challenging due to its water solubility, thus, when aiming at preparing an iron oxide supported catalyst, either pretreatment of the substrate and/or chemical interactions between substrate and iron oxide should be considered. Various different substrates have been tested and reported in literature: inorganic materials, Nafion® membranes, poly-acrylic acid, activated carbon, collagen natural fibers and polymeric films [22–29].

Polymer films are an attractive substrate for antibacterial purposes as they are low-cost, flexible, resistant and widely available, even from recycling practices. Moreover, the issue of bacterial biofilms forming on synthetic polymeric surfaces could be reduced with antibacterial coatings [30]. An iron oxide deposition method on polymer surfaces by direct current magnetron sputtering (DCMS) was previously reported to be active in bacterial inactivation mainly under visible light [31]. Nevertheless, it required expensive state-of-the-art instruments to be achieved.

Most of iron oxides surfaces are positively charged at neutral and acidic pHs, their point of zero charge is around pH 8 [32]. Thus, the presence of electron donor groups, or negatively charged groups on the substrate's surface would induce a stronger attachment and a performing material over several use cycles. It is worth noting that the surfaces of certain polymer films can be smooth and/or lacking of functional groups in their structure; polyethylene for instance, hence the strong attachment of particles on its surface can be problematic. For addressing this issue, several pretreatments have been implemented to generate carboxylic and hydroxyl groups on the surface: Radio Frequency plasma (RF-plasma), Vacuum ultraviolet (V-UV), functionalization via photo-Fenton oxidation or TiO_2 photocatalysis, and acidic pretreatment. However, all these methods require either the use of specialized equipment and/or an important use of energy and resources [28,33].

This is the first work in this field that uses supported iron oxides for bacterial disinfection in both indoor or outdoor conditions, and its high potential impact on health protection because of its cheap and easy-to-apply proposed method of deposition. More specifically, we propose the preparation of polymeric antibacterial films by: a) using visible- and solar light- active iron oxides as semiconductors, b) applying easy and accessible pre-treatment methods (sandpaper scratching and acetone dissolution) and c) following simple preparation techniques (dip-coating and spray-coating). Without neglecting the inactivation mechanisms, we provide a systematic evaluation of different iron sources, pretreatment methods, and deposition techniques and substrates; a combination of factors that lead to materials that can be prepared in any location, especially in places where resources can be scarce.

2. Materials and methods

2.1. Reagents, polymeric substrates, and materials for pretreatment

The source of iron for the coatings was either iron (III) chloride hexahydrate ($FeCl_3 \cdot 6H_2O$, ≥ 99%, Sigma-Aldrich) or soil from an iron mine in Colombia; some of its characteristics can be found in Supplementary material S1 [34]. The substrates for deposing the FeOx were: Polyethylene Terephthalate (PET), 0.05 mm thick, (Goodfellow Cambridge Limited, Huntingdon, UK, reference: ES301250/45), Low Density Polyethylene (LDPE), 0.1 mm thick, (Goodfellow Cambridge Limited, Huntingdon, UK, reference: ET311201) and Polyurethane (PU) (BASF, Lemförde, Germany, reference: 695AIO).

The commercially available materials for pretreatment were: chemically pure zcetone Presto® (Motip Dupli AG, Fehraltorf, Switzerland) and abrasive paper (sandpaper) with two CAMI Grit designations corresponding to different grain sizes: 120 (115 µm) & 60 (265 µm); (Emil Lux GmbH & Co. KG, Wermelskirchen, Germany).

Applying the sandpaper 120 pretreatment (115 µM grain size) to PET-FeOx films led to more homogeneous appearance than PET-FeOx pretreated with sandpaper 60; the latter created deeper non-uniform slits on the PET. For this reason only PET substrates pretreated with sand paper 120 were considered for this study. For PU on the other hand, sandpaper 60 allowed better surface morphology modification.

2.2. Polymer-FeOx film preparation

2.2.1. Dip-coating

The polymeric film substrate (dimensions 25 cm x 7 cm) was washed prior to deposition with demineralized water to remove dirt. Once dry, it was fixed to a metallic coil and immersed in 500 mL of $FeCl_3$ solution in 1-L beakers. This system was magnetically stirred to ensure optimum contact between the surface of the polymeric film and the iron solution. Heating was applied to the solution when necessary by using a hot plate, and the temperature was periodically controlled with a thermometer to keep it constant. Once the predetermined coating time had passed, the films were removed from the iron solution, dried at room temperature (22 °C) and washed with demineralized water to remove the loosely-attached iron oxide and dried, again at room temperature.

2.2.2. Spraying

The polymeric film substrate (dimension 13 cm x 18 cm) was washed with demineralized water, dried and fixed to the bottom of a rectangular Pyrex glass. Subsequently, $FeCl_3$ solution (20 g/L) was uniformly sprayed onto the polymeric film from a 10-cm distance. Next, water evaporation was achieved by placing both the glass and the polymeric film inside an Atlas SUNTEST XLS + solar simulator for 1 h. After water evaporation, the films were sprayed again and placed back in the solar simulator for 1 h more. The latter procedure was repeated 6 times (6 sprays). Lastly, the Polymer-FeOx films were washed with demineralized water to remove the loosely-attached iron and dried at room temperature.

2.3. Pretreatment methods

The following pretreatment techniques were applied to the polymeric films to induce roughness on the substrate and enhance the anchoring of Fe-species:

2.3.1. Physical pretreatment with sandpaper

The surface of the polymeric films was uniformly scratched with sandpaper after previous washing and drying. After this physical pretreatment, the polymeric film was washed and dried again at room temperature.

2.3.2. Acetone

After washing and drying of the polymeric films, they were dipped in non-diluted acetone for 30 min. Subsequently, the films were dried at room temperature, washed with demineralized water and dried again before proceeding with the iron coating.

2.4. Evaporator and irradiation sources

As evaporator, a Suntest solar simulator XLS + (Atlas GmbH, Hanau, Germany) was used after the polymers' coating. It was also equipped with a Xenon lamp and the temperature in its interior part was < 38 °C when the simulator was running.

For indoor light simulation a cavity equipped with 827 Lumilux® Interna (Osram GmbH, Munich, Germany) fluorescent lamps, with a color temperature of 2700 K, and a color rendering index Ra > 80. This simulator mostly provides visible light; the intensity was set at 100 W/m^2 and the light distribution is presented in Supplementary figure S2. The predominant wavelengths are around 610 nm, 550 nm, and 440 nm.

The equipment for bacterial inactivation in outdoor conditions (solar light simulation) was a Suntest solar simulator CPS (Atlas GmbH, Hanau, Germany) equipped with a Xenon lamp, and a cut-off filter to block the light < 290 nm, and with a light intensity of 1000 W/m^2. The light distribution of the Xe lamps is presented in Supplementary figure S3.

The samples were placed 16 cm below the lamps, on a reflecting surface, for both the irradiation simulation and the water evaporation step of the spray coating preparation.

2.5. Bacterial preparation and assessment of antibacterial properties

The details of the bacterial culture have been previously reported by our laboratory [35,36]. Briefly, the strain of *Escherichia coli* (wildtype *E. coli* K12) was used to assess the bacterial inactivation properties of the prepared films and it was obtained from Deutsche Sammlung von Mikro-organismen und Zellkulturen GmbH (DSMZ), Braunschweig, Germany. The agar for plating and subsequent counting of the bacteria was purchased from Merck GmbH, Microbiology division KGaA, (catalogue No.1.05463.0500). The freshly prepared bacterial solution (working solution) used for antibacterial experiments had a bacterial concentration of 10^6 CFU/mL, and was prepared with water containing NaCl/KCl (8 g/l NaCl and 0.8 g/L KCl) from a 10^9 CFU/mL bacterial stock solution. The use of the gram-negative *E. coli* as a bacterial indicator does not cover all conditions of air- and water-borne pathogens that could be inactivated with this work but represent well the coliforms and a first approach to airborne bacteria [37–43].

The polymer-FeOx films, with 1.5 cm x 1.5 cm dimensions, were placed inside glass petri dishes and a droplet of 100 µL of the previously described *E. coli* working solution was deposited on them, subsequently, the petri dishes were closed with a lid to prevent evaporation and located inside the light irradiation sources. After pre-determined irradiation times, the droplet and the film were transferred into a sterile Eppendorf tube containing 900 µL of saline solution. The tube was vortexed for 2 min to ensure detachment of all bacteria from the film and serial dilutions of the vortexed solution were prepared. For the enumeration of bacteria by plating, 100 µL samples of the dilutions were spread onto Plate Count Agar following the standard plate method. Lastly, the plates were incubated for 24 h at 37 °C for allowing colonies' growth to subsequently proceed with their counting. Two aliquots of the samples were plated, including two biological and two statistical replicates, so the reported results correspond to average of the accounted bacterial colonies and their respective standard deviation in the error bars.

2.6. Characterization of the polymer-FeOx films

X-ray photoelectron spectroscopy (XPS) was carried out in an AXIS NOVA photoelectron spectrometer (Kratos Analytical, Manchester, UK) provided with monochromatic AlKa (hv = 1486.6 eV) anode. The reference for the peak positions of Ti, C, O and Cu was the carbon C1s at 284.6 eV [44–46].

2.7. Microscopic analysis

The optical microscopy images of FeOx/PET samples under visible light illumination were collected with using a custom-designed setup, which consisted of an inverted epi-fluorescence microscope (TC5500, Meiji Techno, Japan) and a digital non-cooled CCD camera (Infinity 2, Lumenera Co., Ottawa, Canada).

3. Results and discussion

3.1. FeOx deposition by dip coating and the effect of temperature

The first evaluated deposition method was dip coating using PET as substrate. The conditions set for obtaining different kinds of dip-coated PET-FeOx are shown in Table 1 and the results indicating the effect of deposition temperature are shown in Fig. 1.

The "Blank controls" (uncoated PET under irradiation) showed negligible bacterial inactivation under indoor light (Fig. 1(I)) and 1 log reduction of *E. coli* concentration under solar simulated light (Fig. 1(II)) due to the direct UV light action on the cells. Under indoor light irradiation, a PET-FeOx deposition at a deposition temperature of 50° led to a 2.5 log decrease in *E. coli* concentration. Under solar light, total inactivation was achieved for PET-FeOx films prepared at 50 °C and 40 °C, with slower kinetics for the latter. PET-FeOx prepared at room temperature (22 °C) but with longer deposition time (24 h) seems to induce total bacterial inactivation before 60 min, with slightly lower kinetics than the one induced by PET-FeOx prepared at 40 °C.

Previous studies about iron oxides produced from $FeCl_3$ solutions reported that preparation parameters as reaction time and temperature greatly influence the shape, size and stoichiometry of the formed particles; moreover, it was shown that the solids formed from iron solutions containing chloride were mainly β-FeOOH or α-Fe_2O_3 (akaganeite and hematite respectively). The same study reported that the isoelectric point of these oxides was 7.3 for β-FeOOH and ranging from 6.0 to 6.6 for α-Fe_2O_3 [47]. However, given the temperatures that have been set

Table 1
Conditions tested when dip coating PET films into $FeCl_3$ solution.

Pretreatment (before dip coating)	Deposition Temperature (°C)	Deposition time (h)	Iron chloride concentration (g/L)
None	50	4	20
	50	2	20
	50	4	10
	RT	4	20
	40	4	20
	38 (in evaporator)	4	20
	38 (in evaporator, in the dark)	4	20
	50	4	20 (Natural iron)
SP 120	50	4	20
	RT	4	20
	RT	24	20
	50	4	5 (Natural iron)

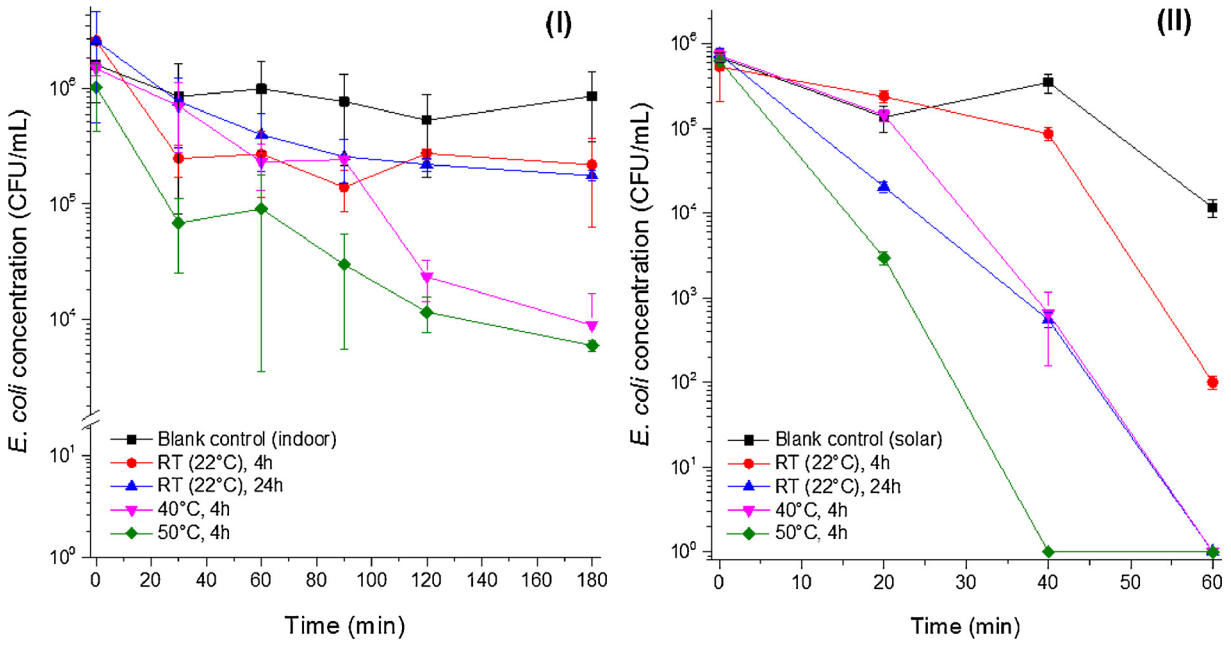

Fig. 1. Effect of deposition temperature on the antibacterial performance of PET-FeOx prepared by dip coating (20 g/L solution of $FeCl_3$). Bacterial inactivation under indoor (I) and simulated solar light (II). Room temperature was 22 °C. *(Note the scale in Fig. 1(I), clearing the trend in the first 2 log units).*

in the present study, the portions of Fe_2O_3 are expected to be low [48]. The dilution of ferric chloride in water leads to its hydrolysis until the formation/precipitation of $Fe(OH)_3$; if the system is heated the formation of Fe_2O_3 is also favored according to Eq. (1).

$$2Fe(OH)_3 \rightarrow Fe_2O_3 + 3H_2O\ \Delta S^{\circ}_{298} = +88\ J/mol\text{-}K \quad (1)$$

The enthalpy of formation of Fe_2O_3 is negative (-824.2 kJ/mol) and given $\Delta S^{\circ}_{298} > 0$, the formation of ferric oxide is spontaneous ($\Delta G = \Delta H - T\Delta S$, is negative); moreover increasing the temperature leads to the decomposition of $Fe(OH)_3$ towards Fe_2O_3. $Fe(OH)_3$ is not thermodynamically stable, thus during its decomposition partially dehydrated intermediates will be formed [49].

The results in Fig. 1 suggest that the enhanced antibacterial performance of a PET-FeOx prepared at 50 °C than the lower temperatures is an indication that the β-FeOOH or α-Fe_2O_3 present in the coating has a better defined particle shape and size. Both particle size and shape are known to have an effect on the activity of the catalysts, smaller/well-defined particles lead to higher catalytic activity.

The performance of the films in Fig. 1 could be the product of a combination of LMCT reaction Eq. (2) and Fe_2O_3 or FeOOH semiconductor action (2.2 and 1.95 eV as band gap respectively) Eqs. (3)–(7) [50].

$$Fe\text{-}(OH)^{2+} + hv \rightarrow Fe^{2+} + OH^{-} + HO^{\cdot} \quad (2)$$

$$Fe_2O_3 + hv \rightarrow Fe_2O_3\ (e^{-} + h^{+}) \quad (3)$$

$$e^{-}_{(cb)} + O_2 \rightarrow O2^{\cdot -} \quad (4)$$

$$h^{+}_{(vb)} + O_2^{\cdot -} \rightarrow {}^1O_2 \quad (5)$$

$$e^{-}_{(cb)} + Fe^{3+} \rightarrow Fe^{2+} \quad (6)$$

$$h^{+}_{(vb)} + L_{ad} \rightarrow L_{ad}^{\cdot +} \quad (7)$$

In the aforementioned reactions, OH^- acts as a Lewis base, giving place to complexation and reduction of ferric iron to ferrous iron. Regarding the semiconductor action, the generated hole can oxidize components of the bacterial cell (Eq. (7)) and additionally, some components of the bacterial cell wall can also act as the ligand binding iron leading to their oxidation by following a LMCT reaction as well (Eq. (8)).

$$Fe^{3+}\text{-}L + hv \rightarrow Fe^{2+}\text{-}L^{+} \quad (8)$$

The replacement of ferric iron by ferrous iron on the surface is expected to be reverted by the oxidation of ferrous iron in contact with environment moisture (Eq. (9)) or by dissolution of ferrous iron in the moisture, making ferric iron available again in the iron coating.

$$Fe^{2+} + 1/4\ O_2 + 2OH^{-} + 1/2\ H_2O \rightarrow Fe(OH)_3\ [51] \quad (9)$$

The bacterial inactivation also relies on the amount of available iron oxide to produce reactive species. Therefore, performance improvement can be also related to greater amounts of FeOx present in the PE-FeOx film and accessible to bacteria, this can be a consequence of both higher temperature and higher deposition time. However, even if deposition times are long (24 h) total bacterial inactivation is not attained by the action of the present iron species under indoor light. This could be related to the lower light intensity, shadowing effect or low light absorbance.

PE-FeOx films deposited at room temperature and tested under simulated solar light (Fig. 1(II)) showed that, if deposition times are long (24 h), the iron species induce total bacterial inactivation; this as consequence of phenomena combination: LMCT reaction (Fe^{3+} availability), semiconductor action (more energetic photons are available due to UV-portion of solar light), higher light intensity and UV-action on the cells. In addition, it is possible that besides these modes of action, the iron leaching from the coating to the interior of the *E. coli* cells triggers an internal photo-Fenton, eventually leading to its inactivation. Also, according to the previous indications, the iron coatings deposited at room temperature possibly present an amorphous shape, which could slightly compromise the semiconductor activity but apparently, not the ligand-to-metal-charge-transfer (LMCT) reaction that leads to the generation of ROS for the subsequent bacterial attack.

Other PET-FeOx films were obtained by keeping the deposition temperature at 50 °C, applying different coating times (4 h or 2 h) as well as fixing different $FeCl_3$ solution concentration (10 g/L or 20 g/L). Matijević and Scheiner have already reported the effect of temperature, concentration of the iron source, and its nature in particle size, morphology and types of produced iron oxides [47]. In this study, the films prepared with 20 or 10 g/L of $FeCl_3$ solution with a deposition time of 4 h led to ~3 log units *E. coli* concentration reduction under indoor

irradiation and both of the films led to a total bacterial inactivation in 40 min under simulated solar light. The film prepared with 10 g/L $FeCl_3$ solution induced slightly slower action. Keeping the $FeCl_3$ solution concentration at 20 g/L and reducing the deposition time to 2 h led to an inactivation similar to the one induced by the aforementioned films both under indoor irradiation and simulated solar irradiation. In conclusion, the set range of parameters' variation for these tests had not a big impact in modifying the antibacterial performance but for a wider range of variations, evidence of the effect is expected to be clearer. These results are presented in Supplementary figure S4.

A previous study addressing a similar dip-coating technique for the preparation of PE-FeOx films led to coatings with a RMS of 78.4 nm [29]. These non-pretreated LDPE-FeOx films showed rod-like aggregates growing in random directions, this was determined by AFM. The morphology of the obtained FeOx-coating was characterized by a closely packed contour, which would allow more contact points with the targets. An adapted figure schematizing the contact between bacteria and FeOx coating is shown in Supplementary figure S5.

Modifying the substrates' morphology not only would induce changes in the FeOx-coating contours but would also allow higher FeOx fixation. Moreover, two more things have to be taken into account: a) that PET has carboxylic groups in its structure, b) the pH of the suspensions was always acidic (~2.5) after $FeCl_3$ dilution, which would induce positively charged FeOx particles regardless their nature; both β-FeOOH and α-Fe_2O_3 are positively charged at pH values below 6. The aforementioned two conditions would prompt Van der Waals interactions between PET's surface and the positively charged iron oxide particles.

3.2. Dip-coating: effect of substrate's pretreatment (sandpaper and acetone), deposition time and use of natural iron

3.2.1. Effect of pretreatment (sandpaper and acetone)

Acetone and sandpaper pretreatment of PET were addressed with the purpose of modifying the substrate's surface morphology increasing the iron oxides fixation and inducing roughness; the results showing their effect are shown in Fig. 2.

Dark controls for PET-FeOx were performed on non-pretreated films and had no major effect. The sandpaper pretreatment induces higher amounts of deposited iron and in dark conditions the bacteria would be in contact only with the outer FeOx layers. Thus, light would be definitely necessary to create an electron/hole pair, to induce LMCT reactions or to lead to an intracellular inactivation by augmented Fe import.

Fig. 2(I) shows that sandpaper pretreatment of PET films dip-coated with $FeCl_3$ (20 g/L) for 4 h at 50 °C has no major effect on bacterial inactivation under indoor conditions, however, acetone pretreatment enables the films to attain total bacterial inactivation before 180 min. Under simulated solar light (Fig. 2(II)), when comparing the bacterial inactivation of sandpaper and acetone pretreated PE-FeOx with non-pretreated PET-FeOx, the first two seem to induce slightly higher kinetics, making more evident the effect of modified morphology. The acetone pretreatment is expected to induce roughness on the PET surface by partially dissolving it; this by getting into small crevices the PET might have in its surface. We also expect that these particular morphology changes would generate more compatible contact points between the coating and the bacteria (in terms of size).

It is worth noticing that even with lower light intensity and less energetic wavelengths (indoor light irradiation (Fig. 2(I))), a simple pretreatement as sandpaper scratching for preparing PET-FeOX at 50° induces a bacterial concentration reduction of 3 log units following a close to linear trend. Based on this, total bacterial inactivation could be attained after ~6 h irradiation, provided that the accumulation of dead cells on top of the coating does not block the indoor light.

3.2.2. Effect of sandpaper pretreatment and deposition time

For comparison with results from Fig. 1, PET-FeOx samples were also prepared at room temperature (22 °C) with and without sandpaper pretreatment of PET. Under indoor irradiation the films prepared at room temperature had a more modest performance than the ones prepared at 50 °C regardless their previous sandpaper pretreatment and longer deposition time (Fig. 2(I)). Regarding simulated solar light, the bacterial inactivation performance seems to improve when addressing sandpaper pretreatment and deposing at room temperature. Total bacterial inactivation is not attained before 60 min with "Non-pret, RT

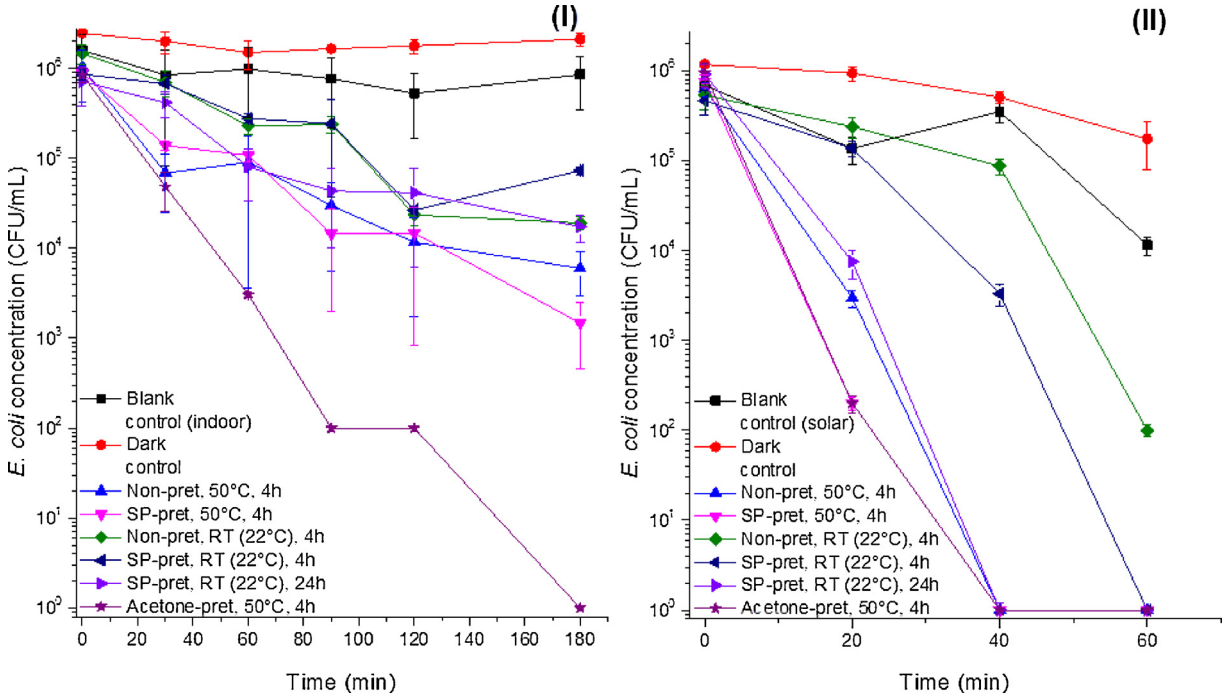

Fig. 2. Effect of PET's pretreatment and deposition time on the antibacterial performance of PET-FeOx prepared by dip coating. Bacterial inactivation under: indoor light (I) and simulated solar light (II).

(22 °C), 4 h" while for "SP-pret, RT (22 °C), 4 h" it is seems to be attained before 60 min. Moreover, if sandpaper pretreatment is addressed while depositing at room temperature for longer time (24 h), the bacterial inactivation could be attained before 40 min. These results indicate that in absence of a modest temperature treatment (50 °C), higher amounts of FeOx anchored on the substrate or enhanced roughness due to physical pretreatment lead to improved activity.

Sandpaper pretreatment increased the surface roughness and improved the homogeneous appearance of the PET-FeOx films prepared by dip coating. Moreover it could save deposition time when deposing at room temperature or it could be addressed for avoiding heating if longer deposition times are set.

The deposition temperatures set in our preparation techniques are low (room temperature up to 50 °C) and this would lead to a type of film growth described by Movchan and Demchishin as *zone I* [52]. In this zone, the adatoms mobility is reduced and structures with fine fiber texture develop, columns preserve the random orientation of the nuclei and surface roughness develops, leading to extensive porosity [53].

Former studies have presented other ways for modifying a polymer's surface by plasma pretreatment or UV-C light pretreatment. It was reported that UV-laser pretreatment of polymers' led to the enhancement of their roughness thus improving the adhesion of the subsequent coating [33]. RF-plasma pretreatment has been previously addressed in our lab and it showed to improve the performance of films for inducing bacterial inactivation [31].

In this work, we demonstrate that simple, low-cost pretreatment methods such as sandpaper pretreatment or acetone pretreatment of PET can easily modify the morphology of the coatings (more contact points with bacteria) and suspect that allow higher amounts of FeOx to be anchored, with beneficial action towards their inactivation. For instance, sandpaper pretreatment of PET for dip-coating at 50 °C during 4 h leads to a 35% increase of the rate constant k_{obs} compared to the non-pretreated PET-FeOx prepared under the same conditions. Regarding room temperature dip coatings, sandpaper pretreatment also leads to reduction of exposure time, further supporting the efficacy and applicability of the proposal.

In order to verify the composition of the presented films, analysis of selected samples took place by XPS. Table 2 shows the surface atomic distribution of elements on the PET surface after FeOx deposition. It is readily seen that FeOx was detected at the surface of samples. This can be attributed to the aggregation of iron species during the deposition leading to large voids and non-homogeneous distribution of the coating. Oxygen was detected in all the samples revealing oxidized iron species. Surprisingly, S2p was found in all samples as well as Cl2p. This may be due to the cross contamination, samples handling and the purity of the purchased iron species.

X-ray photoelectron spectroscopy (XPS) was also used to further investigate the Fe oxidation state on the surface of FeOx-PET. Fig. 3 shows the survey spectra of the coated Fe surfaces. Peaks representing species containing Fe, C, O, and Cl on the surface are present for the treated PET-surfaces. The signal of Cl indicates that some of the FeCl or

Table 2
XPS derived surface atomic percentages.

Element	Samples			
	Acetone PET Dip Coating (50 °C, 4 h, 20 g/L)	SP120 PET Dip Coating (50 °C, 4 h, 20 g/L)	PET Dip Coating (50 °C, 4 h, 20 g/L)	PET Dip Coating (RT, 4 h, 20 g/L)
C1s	74.76	46.13	43.78	52.75
N1s	3.07	0	1.71	1.29
O1s	19.23	37.15	36.19	33.16
Na1s	0.66	1.59	0.91	0.8
S2p	0.36	0.31	1.44	0.17
Cl2p	0.24	1.74	1.73	1.27
Fe2p	1.68	13.09	14.24	10.56

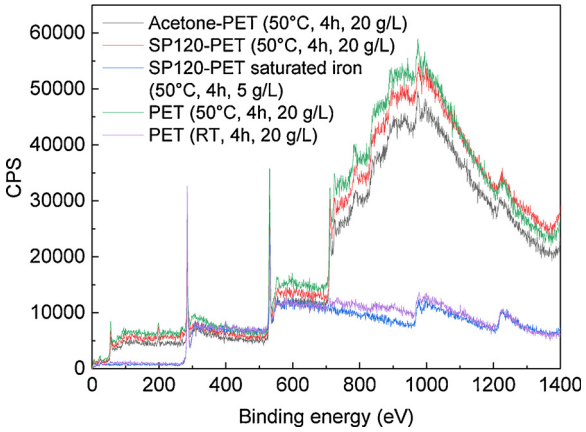

Fig. 3. XPS survey of the different FeOx preparations.

$FeCl_2$ remained on the surface. An X-ray induced Auger Na KL2,3L2,3 peak at BE of 496.7 eV, and a Na1s peak at BE of 1071.8 eV (positions determined with CasaXPS) are present in all samples with surface atomic percentages from 0.66 to 1.59%.

The Fe2p XPS-peaks deconvolution are shown in Fig. 4. The source of O1s mainly comes from the oxidized Fe. Oxidized atmospheric species (adventitious carbon species – sometimes attributed to contamination) could adsorb on the Fe-PET surfaces during samples preparation and drying. Organic molecules could also oxidize on the surface after their adsorption on the Fe surface, thus contributing to the peaks of Fe/O_2. The source of the O1s signal can also come from the water molecules that remained on the surface after sample drying/exposition to ambient humidity. A discussion of which species containing oxygen are the most probable on the surface will be given below. The presence of the C1s is a strong indication that: (i) the surface distribution of iron during the deposition was not homogeneous, (ii) the C-molecules were adsorbed on the surface before pretreatment and coating arising from the adsorbed carbonaceous species i.e. contamination.

It is readily seen that at high bending energies Fe2p or Fe3p are both found. The relative intensities of these peaks depend on the depth of the iron with respect to the surface. Sample roughness can greatly change the Fe-peaks relative intensities as recently reported by our laboratory [54].

In Fig. 4, it is also seen that the core level lines are accompanied by satellite structures showing almost similar trends and positions for the different FeOx-PET coatings. Normally, these satellites originate from shake processes revealing an electronic excitation to unoccupied states. Therefore, the satellite structures of the iron can be correlated to the O1s, Cl2p or S2p states. The little shift observed for these satellites shows changes in the degree of covalence. More information about the electronic structures could be derived from the measurement of the energy loss of the satellites compared with theoretical calculations, but it is currently out of the scope of this work.

3.2.3. Use of iron mine soil as natural iron source

With the purpose of preparing an even more simple-accessible material, mineral iron from a mine was chosen to replace chemical grade $FeCl_3$ and continue addressing the dip coating method. The type of soil used in this work was used in previous studies and it was chosen due to its high iron oxide content [34].

PET-FeOx(NatIron) films were prepared by dip coating non-pretreated PET in a 20 g/L red soil suspension at 50 °C, during 4 h. When sandpaper pretreated PET was used, it was dip-coated with a 5 g/L red soil. Their bacterial inactivation performance is shown in Fig. 5. When no pretreatment of the PET was addressed before coating, the decrease in *E. coli* concentration induced by the PET-FeOx films was less than 1 log unit for indoor irradiation (Fig. 5(I)) and 2 log units under solar

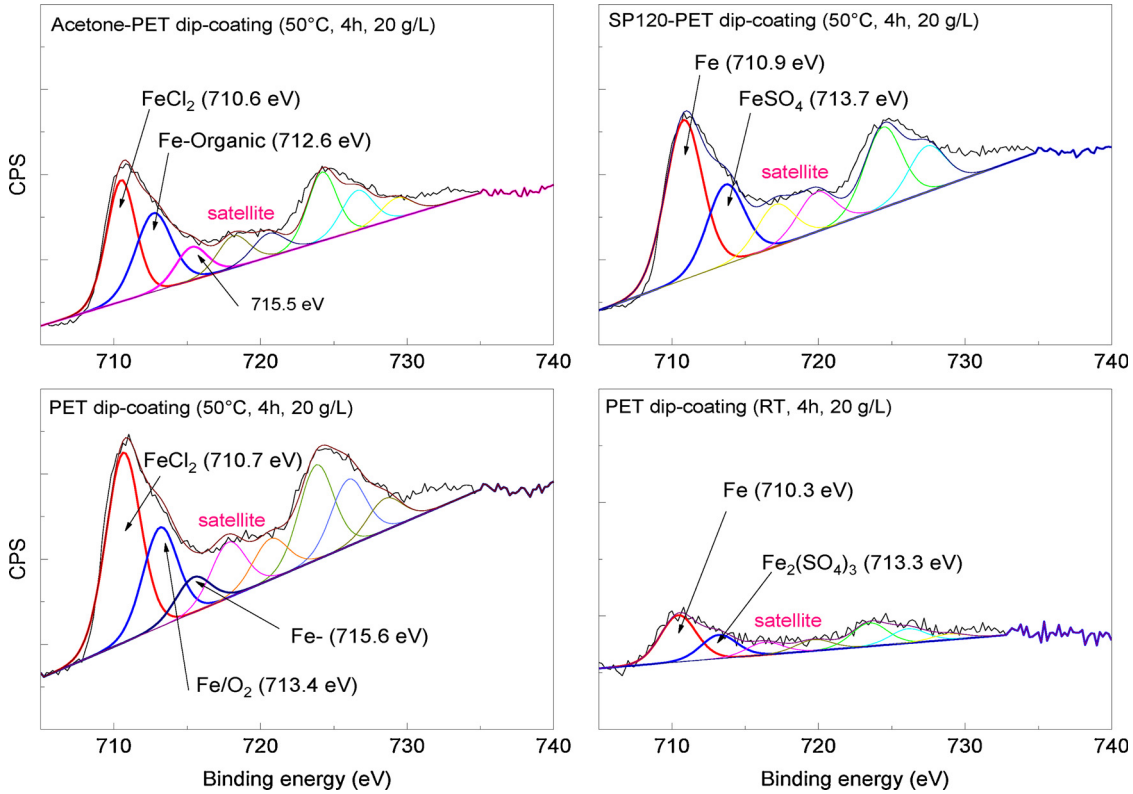

Fig. 4. FeOx deconvolution of the different FeOx-PET coatings.

simulated light (Fig. 5(II)). The sandpaper pretreatment of PET before dip coating lead to no significant variation of performance under indoor light (Fig. 5(I)), however it seemed to enable total bacterial inactivation in 1 h under solar irradiation (Fig. 5(II)).

The bacterial inactivation of sandpaper pretreated PET-FeOx (NatIron) under solar simulated light is slower than the one of "SP-pret, PET-FeOx, 50 °C, 4 h" (Fig. 2(II)) prepared with $FeCl_3$ as iron source (total bacterial inactivation in 40 min). The used source of natural iron contains 81.26% iron, lower percentages (below 7%) of Al, Si and P; it has a modest specific surface area (19.97 m^2/g) and presented a particle size of approximately 1.2 µm [34]. The slower kinetics and longer inactivation time induced by the films prepared with this iron source are related to the aforementioned characteristics; the particles' attachment can be compromised and the other components (different than iron) can interfere as well.

Once again we have signs of the positive effect of the sandpaper pretreatment, most probably due to the higher amounts of deposited FeOx. Summing up, it can be established that the use of natural iron for

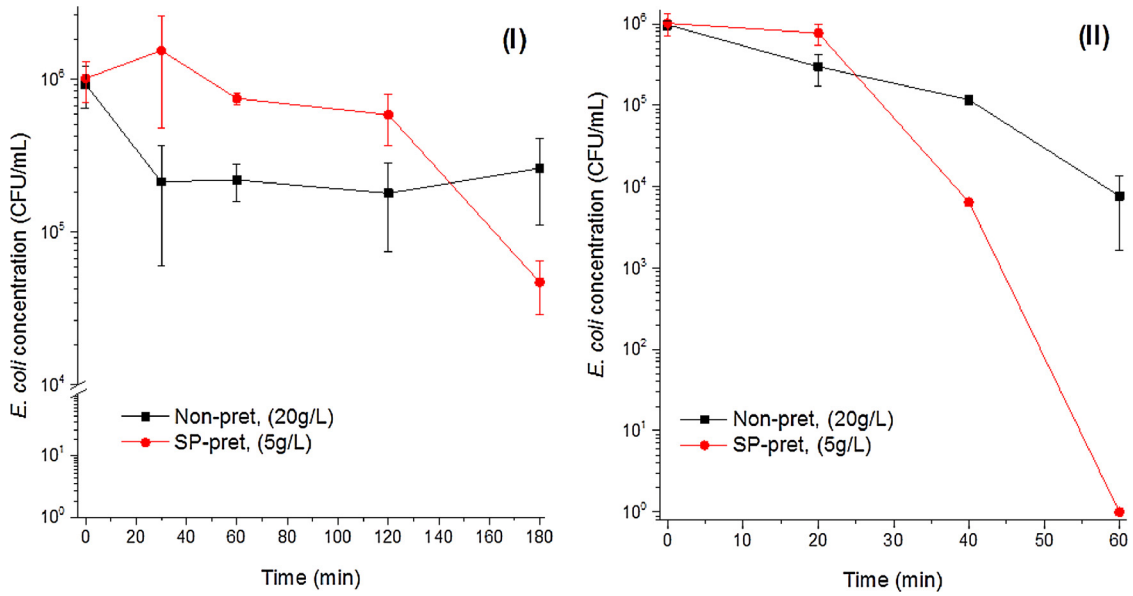

Fig. 5. Antibacterial performance of PET-FeOx films prepared by dip coating with a 20 g/L natural iron suspension. Deposition at 50 °C during 4 h. Physical pretreatment with sandpaper 120. Bacterial inactivation under: indoor light (I) and simulated solar light (II). *(Note the scale in Fig. 3(I), clearing the trend in the first 1.5 log units)*.

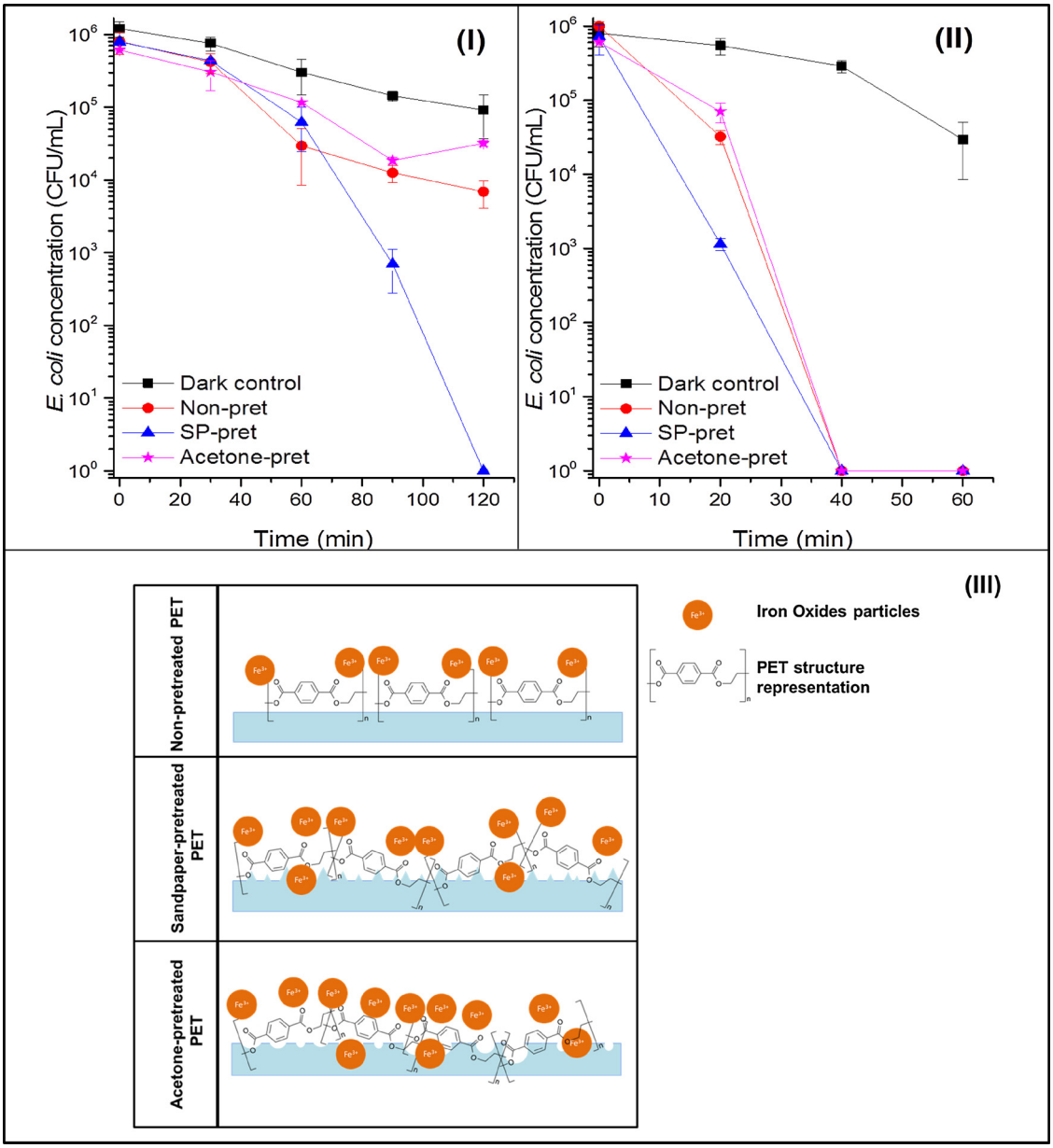

Fig. 6. Antibacterial performance of PET-FeOx films prepared by spray coating (20 g/L $FeCl_3$ solution: 6 times in 6 h) and the effect of PET pretreatment (sandpaper 120 and acetone). Bacterial inactivation under: indoor light (I) and simulated solar light (II). (III) Representative scheme of PET pretreatment on its surface.

PET dip-coating is suitable for producing active antibacterial surfaces (under solar light).

3.3. Spray coating and the effect of pretreatment

Spray coating method is retained as simple since it does not require sophisticated equipment other than a spraying bottle and a space for evaporation, therefore it was addressed for preparing antibacterial PET-FeOx films by depositing on: sandpaper pretreated PET, acetone pretreated PET and non-pretreated PET. Moreover, the morphology of the obtained coatings is expected to differ from the one obtained by the dip coating performed in this study.

The antibacterial performance of the PE-FeOx films prepared by spray coating and a schematic representation of the effect of pretreatment on PET are shown in Fig. 6. The dark controls, performed for non-pretreated spray-coated PET-FeOx, revealed that after 3 h contact only a 1 log decrease of the bacterial concentration was attained. When irradiating with indoor light, non-pretreated spray-coated PET-FeOx led to a 2 log decrease in *E. coli* (Fig. 6(I)). Non-pretreated spray-coated PET-FeOx present a less spread coating, it is rather concentrated in spots, unlike the more uniform appearance given by the dip coating method. Acetone pretreated spray-coated PET-FeOx induced around 1.5 log bacterial concentration reduction and sandpaper pretreated spray-coated PET-FeOx led an *E. coli* shoulder-profiled inactivation curve that suggested total bacterial inactivation before 2 h. This kind of bacterial inactivation tendency has been reported to be caused by “a single-hit multiple-target” or a series of event phenomenon in which the damage to the cell is cumulative rather than instantly lethal [55].

Under solar light simulation (Fig. 6(II)), all of the prepared materials: non-pretreated, acetone pretreated and sandpaper pretreated spray-coated PET-FeOx led to total bacterial inactivation before 40 min with similar kinetics. Under these conditions, the bacterial inactivation induced by the films is way quicker given the more energetic photons activating the FeOx as semiconductor, as well as the mere direct effect of UV-light on the bacterial cells.

The difference in performance under indoor light irradiation

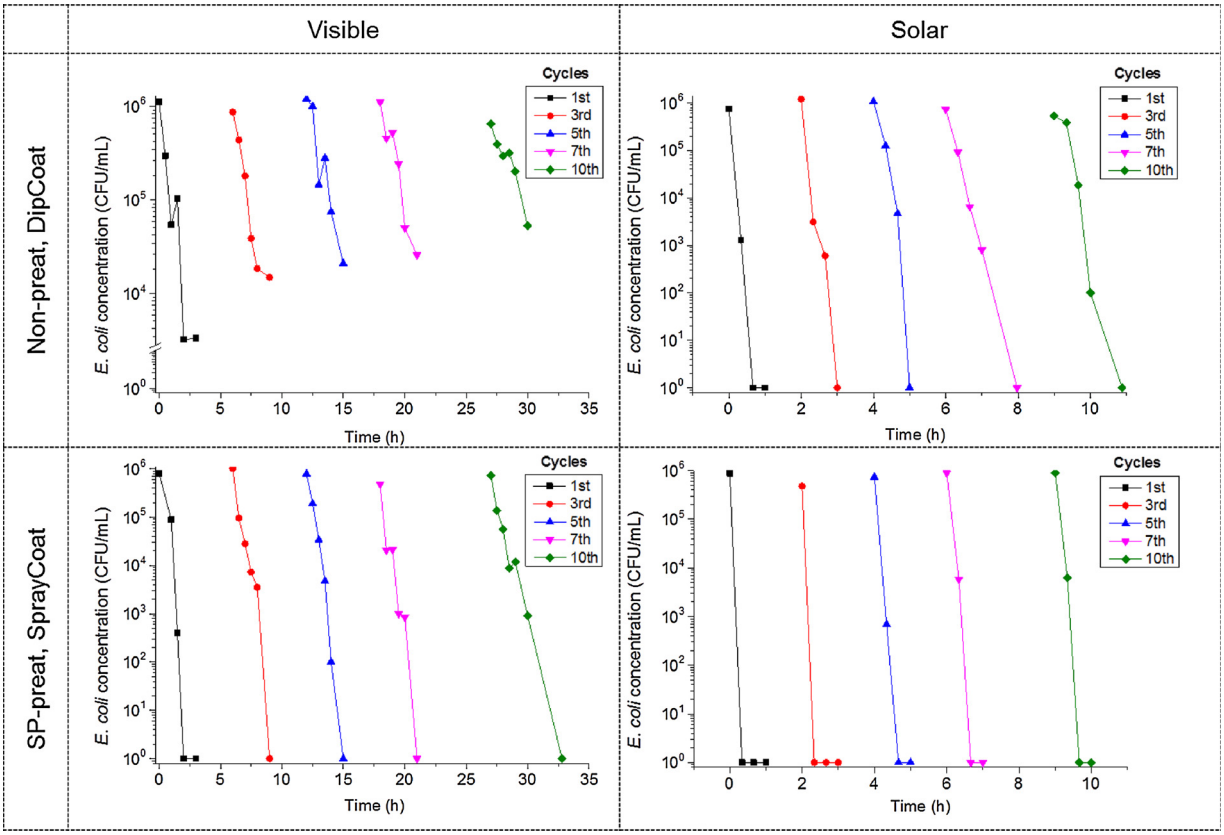

Fig. 7. Comparison of re-used PET-FeOx's antibacterial performance prepared by two different methods: dip coating (Non-pretreated PET, 50 °C, 4 h deposition) and spray coating (sandpaper-pretreated PET, spray with 20 g/L $FeCl_3$ solution: 6 times in 6 h).

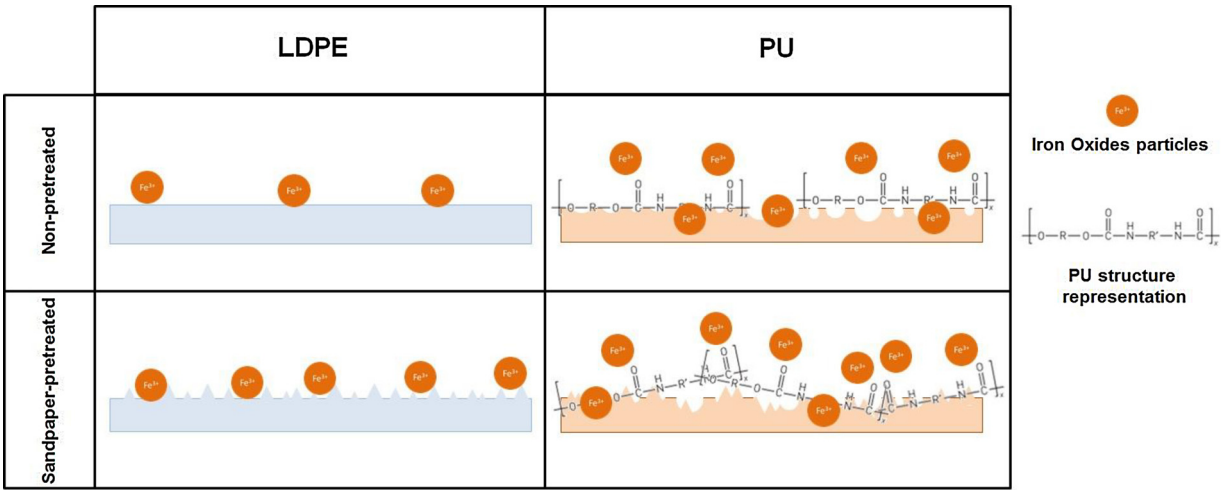

Fig. 8. Schematic representation of the effect of sandpaper pretreatment on PU and LDPE surfaces.

between non-pretreated spray-coated PET-FeOx and sandpaper-pretreated spray-coated PET-FeOx are expected to be related to more rough surfaces and higher amounts of FeOx (Fig. 6(III)). There will be a production of ROS by both semiconductor effect and LMCT reaction; the limitation regarding the LMCT action relies on the depletion of Fe^{3+} available on the surface, which gets reduced to Fe^{2+} during the formation of $HO^{\bullet}$ radicals. However, as these ferrous species are highly soluble in water, they migrate to the bulk of the bacterial solution (droplet) allowing the Fe^{3+} in the inner layer of the FeOx coating to be active again for reaction. In real applications there would be no "bulk" (droplet) only highly available oxygen and adsorbed moisture and in this case we could still consider an oxidation from ferrous to ferric iron.

The growth of films on substrates is known to depend on the ratio of the diffusion rate to the deposition flux: *D/F*. For large values of D/F (deposition slower than diffusion) the film growth takes place allowing the adsorbed species finding a minimum energy configuration (regular molecular self-assembly). Low D/F values on the other hand are related to a fast deposition relative to the diffusion rate, therefore the pattern of growth would be quite random and determined by individual processes, mainly leading to metastable structures [56]. In dip coating it is expected that Van Der Waals interaction would help FeOx particles' "spreading" on the PET surface (enhancing diffusion) and the deposition is low due to the important bulk of solution the particles have to overcome before settling on the PET surface. We suggest our conditions

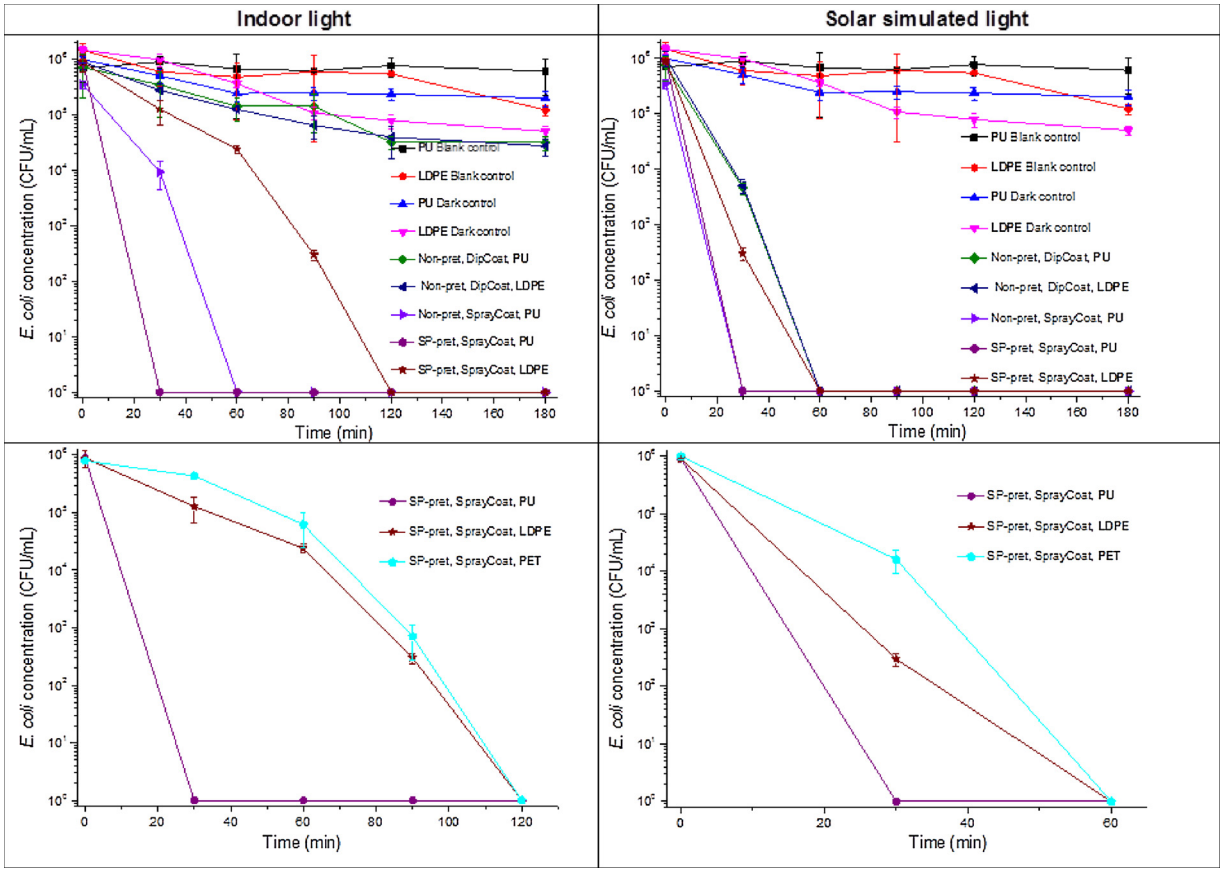

Fig. 9. *Upper part of the figure:* Antibacterial performance of PU-FeOx and LDPE-FeOx prepared by dip coating (20 g/L $FeCl_3$ solution, 50 °C, 4 h deposition) and spray coating (spraying with 20 g/L $FeCl_3$ solution: 6 times in 6 h) with and without substrate's sandpaper pretreatment (120 sandpaper for LDPE and 60 sandpaper for PU). *Lower part of the figure:* Antibacterial performance comparison for sandpaper-pretreated spray-coated PET-FeOx, LDPE-FeOx and PU-FeOx.

lead to an intermediate range of D/F with rod-like (somehow regular) columns growing in random directions, the characteristic type of growth for intermediate D/F ratios [28,31] (also see Supplementary material S5). Consequently, the spray coating is expected to lead to diffusion-limited growth of the coating as the deposition flux is significantly higher than the one happening in dip coating. Also, given that the spray-coating is carried out 6 times, the initially isolated nuclei formed gradually fuse to finally induce a rougher, highly porous coating.

3.4. Reuse of PET-FeOx films

The antibacterial characteristics for PET-FeOx prepared by the two different coating methods addressed in this work after several use cycles was assessed. Dip-coated "Non-pret, PET-FeOx, 50 °C, 4 h" with a 20 g/L $FeCl_3$ solution as iron source was compared to sandpaper-pretreated spray-coated PET-FeOx. This comparison was addressed to compare the robustness of the two basic PET-FeOx films; the corresponding results are shown in Fig. 7.

The bacterial inactivation of the non-pretreated dip-coated PET-FeOx film under indoor light was limited to approximately 2 log units in the process of 10 times reuse. Nonetheless, its re-use performance under solar simulated light is better as total bacterial inactivation is reached within the first hour during the first 5 cycles. The 7th and 10th cycle took twice the time to reach total bacterial inactivation. The decrease of the disinfection rate is probably caused by FeOx loss during each bacterial inactivation cycle since 2 min vortexing of the films was applied to ensure complete detachment of the adhered *E. coli* cells, as well as for the subsequent washing step. This process would not take place in real applications, thus better performances are expected.

The loss of activity of iron oxide coated polymers films as they are submitted to consecutive re-use cycles has been previously reported; bacterial inactivation or organic pollutant degradation became slower after several cycles, thus our results are in accordance with literature [28,31].

Regarding spray-coated sandpaper-pretreated PET-FeOx films and their antibacterial properties under indoor light, the films remain active during 10 use cycles, totally inactivating bacteria in 2 h during the first 7 use cycles. The 10th reuse required 5 h to attain total bacterial inactivation. It is worth noting that besides the absence of vortexing in real applications the sandpaper-pretreatment is expected to enhance the attachment of iron oxide; allowing higher availability of photoactive material to induce bacterial inactivation throughout the reuse cycles.

Spray coating showed a good stability towards recycling, provided that a pretreatment such as sandpaper is applied to help the iron oxide attachment. Moreover, it is expected that more porous FeOx coatings are induced by this deposition method, leading to more contact points between target and photoactive material as previously discussed.

3.5. FeOx deposition on alternative polymer substrates (PU and LDPE) and the effect of their pretreatment with sandpaper

A Schematic representation of the effect of sandpaper pretreatment on LDPE and PU films is shown in Fig. 8. The effect of the substrate composition and its morphology on the iron attachment was briefly evaluated, as well as the efficiency towards bacterial inactivation of the resulting materials.

The PU used for these experiments presented different surface texture on the different sides of the film; the "rough side" was chosen to depose FeOx and to perform antibacterial tests. The roughness of this

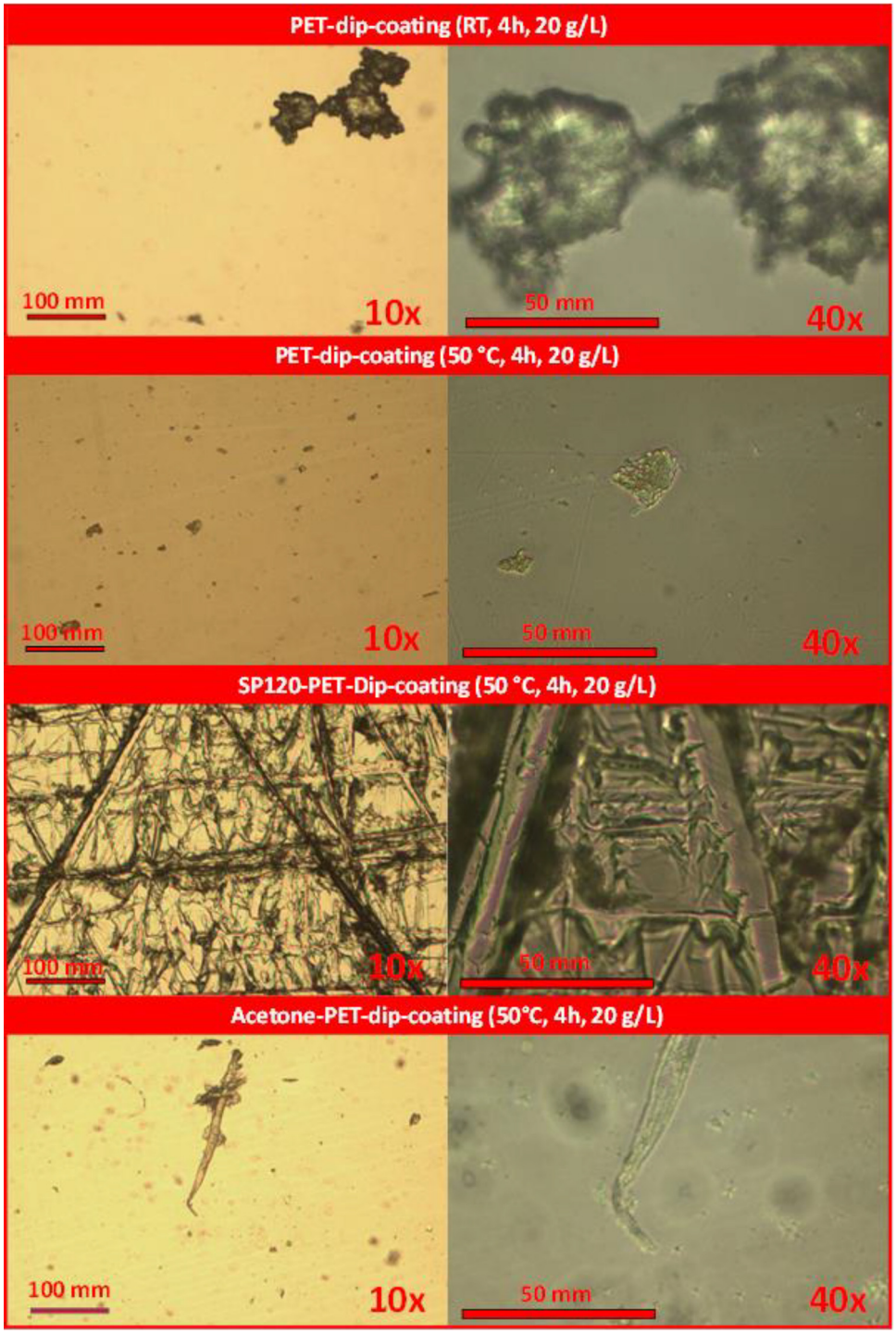

Fig. 10. Microscope imaging on representative antibacterial samples of this work.

substrate would allow the attachment of higher amounts of FeOx and moreover there is the possibility of hydrogen bonds formation between FeOx and carboxylic groups in the PU structure.

Fig. 9 shows blank and dark controls, for the uncoated substrates and for the FeOx-coated substrates respectively; the antibacterial performance of the different prepared films under indoor light and solar simulated light is also shown. Blank and dark controls showed a reduction in *E. coli* concentration of around 1 log unit. Non-pretreated dip-coated PU-FeOx and LDPE-FeOx under indoor light, showed modest decrease in bacterial concentration as well (Fig. 9 upper left part). These films led to similar bacterial inactivation kinetics and a total bacterial inactivation time bellow 60 min under solar simulated light.

Preceding studies comparing dip-coating with iron oxide on different polymeric substrates [28,57] reported that the nature of the polymeric substrate slightly influenced the material's efficiency. Parameters such as the preparation method, temperature or pretreatments might have a greater effect. However, it is worth noting that evidencing the effect of the composition of the polymeric substrate would be more assertive when carrying out the evaluation of the antibacterial performance throughout the material's reuse. The presence of carboxylic groups is expected to mainly contribute to better attachment of the particles; meaning that the particles would stay attached (and active)

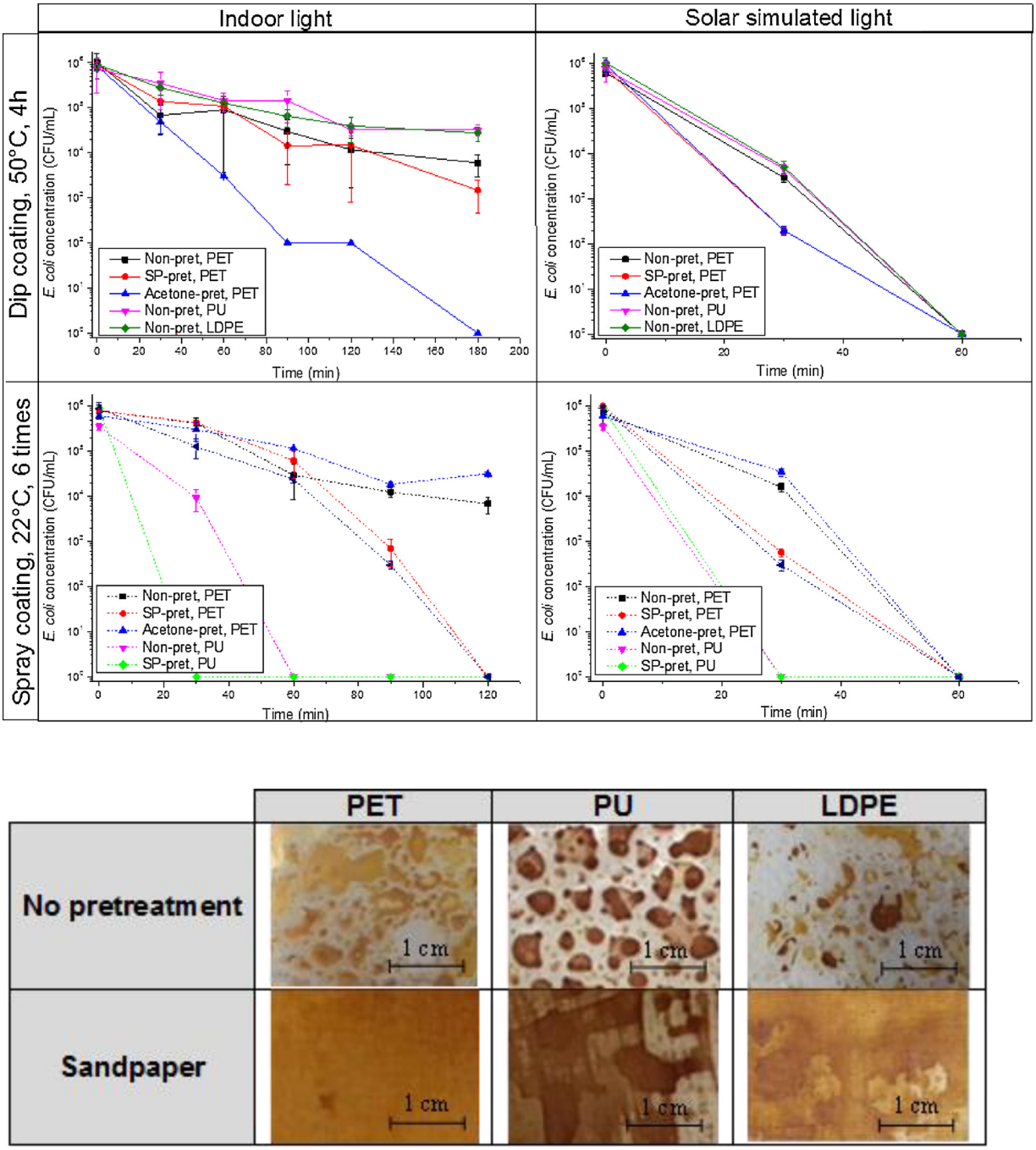

Fig. 11. *Upper part of the figure*: Summary of antibacterial performance for materials prepared by the two different addressed deposition methods on the different used substrates. *Lower part of the figure*: macroscopic evaluation of materials' coating.

for longer use periods.

Spray coating method was addressed for both of the alternative substrates while considering physical pretreatment with sandpaper as well. Bacterial inactivation on non-pretreated spray-coated LDPE-FeOx was not tested due to high inhomogeneous appearance.

Total bacterial inactivation for sandpaper-pretreated spray-coated LDPE-FeOx was reached under both light simulations; before 2 h under indoor light (Fig. 9 upper left part) and before 60 min under solar simulated light (Fig. 9 upper right part). This material also allowed faster bacterial inactivation kinetics than non-pretreated dip-coated PU-FeOx and LDPE-FeOx under solar light. Comparing the performance of sandpaper-pretreated spray-coated LDPE-FeOx with non-pretreated dip-coated LDPE-FeOx, the improvement can still be explained by the greater amount of anchored FeOx and the induced changes in the morphology (regardless the higher deposition temperatures). Additionally, when comparing sandpaper-pretreated spray-coated LDPE-FeOx to non-pretreated dip-coated PU-FeOx the differences in performance most likely rely on morphology; apparently the size of the PU pores does not induce the closely packed "peaks" of FeOx coating that would allow more contact points between bacteria and the antibacterial surface, moreover, the presence of carboxylic groups would show an effect if the performance over several use cycles is assessed.

The differences for spray-coated PU-FeOx films performance are evident; under indoor light (Fig. 9 upper left part), non-pretreated PU-FeOx induces total bacterial inactivation in 60 min, and if sandpaper pretreatment is addressed, this time is reduced to less than 30 min, thus,

modifying the characteristic porous surface of the PU allows higher amounts of anchored FeOx and even the low-energetic photons from the indoor light boost photochemical reactions (semiconductor, LMCT, and internal photo-Fenton). Under solar light simulation (Fig. 9 upper right part), regardless the pretreatment of PU, there is total bacterial inactivation before 30 min as well; most likely bacterial inactivation is reached even sooner as there are more energetic photons enhancing the bacterial inactivation.

The performance of the spray-coated sandpaper pretreated LDPE-FeOx is similar to the one observed for PET-FeOx coated in the same conditions (Fig. 9 lower left and right part). Both are composed of smooth polymeric substrates with physically modified morphology, however, due to the presence of carboxylic groups in the PET, using it as substrate would lead to films performing for longer use cycles. Dip coating technique for the different substrates did not lead to significant performance variations; for spray coating (previous sandpaper pretreated) PU seems to be an optimal substrate for antibacterial applications. It can still perform very well if sandpaper pretreatment is not addressed, as presented in Fig. 8 its morphology and composition induce the attachment of more FeOx and most probably, these particles will be also better attached when comparing to LDPE.

To summarize, for comparison reasons, the microscopic and macroscopic appearance of the spray-coated films is shown in Figs. 10 and 11 the comparison among dip and spray coating, under solar vs. visible light. It can be readily observed how sandpaper pretreatment significantly improves the homogeneity of the FeOx coating, and the strong reduction time in spray coated samples, respectively. Furthermore, in Fig. 10 it is noteworthy to mention some special cases, such as the acetone pre-treated sample, which presents small diffuse aggregates, thus allowing a high film transparency, as well as the SP120-pretreated dip-coated (at 50^0C), whose abrasion permits the adhesion of larger aggregates and a wider iron coverage; these were two of the conditions that led to high antibacterial activity.

4. Conclusions

In this work, simple, low-cost antibacterial polymer-FeOx preparation methodologies were addressed; they comprised accessible and easy to perform deposition methods (dip coating, spraying) and pretreatments of the substrates, namely sandpaper scratching and acetone dissolution. Both pretreatments modified the morphology of the substrate, either by physical abrasive action or by partially dissolving the substrate after getting into small crevices of the polymer. Five of these films induced total bacterial inactivation under both indoor and outdoor environment: acetone-pretreated dip-coated PET-FeOx, sandpaper-pretreated spray-coated PET-FeOx, non-pretreated and sandpaper pretreated spray-coated PU-FeOx and sandpaper-pretreated spray-coated LDPE-FeOx. The performance over several use cycles for films prepared with substrates as PU or sandpaper-pretreated spray-coated LDPE was also noteworthy.

The effect of temperature for dip coating was emphasized; temperatures higher than room temperature boost iron chloride hydrolysis, which subsequently allow the formation of iron oxides with higher antibacterial activity. Even at the mild conditions assayed here, high bactericidal activity was attained. We also showed the potential use of natural iron sources for the preparation of antibacterial surfaces, albeit possible only under solar light. This is of particular interest for applications in locations where soil containing large amounts of iron oxide is more accessible than chemical grade iron.

The spray coating procedure induces the growth of FeOx coatings with morphologies that allow more contact points with the bacteria leading to faster antibacterial actions, allowing coating of larger surfaces. Evidence of the robustness of sandpaper-pretreated spray-coated PET-FeOx was shown, active for bacterial inactivation under indoor and solar light simulated irradiation up to 10 cycles and homogeneous coating appearance.

Our study is an indication of the great potential of application the handcrafted iron coatings deposited on polymeric substrates have, not only for hospital environments but also for daily life environments and objects: bathrooms, handles and furniture (indoor and outdoor). In real applications the bulk of a water droplet would be present mostly by occurrence of rain or present on the film as moisture, a fact that reduces diffusion limitations. Furthermore, iron leaching would not pose a complication for human health due to its acceptability in our organisms; it could even be beneficial for the antibacterial performance. Finally, if the substrates have polar groups in their composition, the susceptibility of the materials to water washing or rain is expected to significantly decrease.

Acknowledgements

Stefanos Giannakis and Cesar Pulgarin acknowledge the financial support provided by the European project WATERSPOUTT H2020-Water-5c-2015 (GA 688928) and the Swiss State Secretariat for Education, Research and Innovation (SEFRI-WATERSPOUTT, No.: 588141). The authors would also like to acknowledge the contribution of Dr. Andrzej Sienkiewicz for the acquisition of the microscopy images.

Appendix A. Supplementary data

Supplementary material related to this article can be found, in the online version, at doi:https://doi.org/10.1016/j.apcatb.2018.10.035.

References

[1] W.R. Sanborn, Am. J. Public Health N 53 (1963) 1279-&.
[2] S.J. Dancer, J. Hosp. Infect. 73 (2009) 378–385.
[3] D.J. Weber, W.A. Rutala, M.B. Miller, K. Huslage, E. Sickbert-Bennett, Am. J. Infect. Control 38 (2010) S25–S33.
[4] G.L. French, J.A. Otter, K.P. Shannon, N.M.T. Adams, D. Watling, M.J. Parks, J. Hosp. Infect. 57 (2004) 31–37.
[5] M.I. Ltd, Microban International Ltd., 2017.
[6] J.J. Curtin, R.M. Donlan, Antimicrob. Agents (2006) 1268–1275 Ch 50.
[7] H.A. Foster, I.B. Ditta, S. Varghese, A. Steele, Appl. Microbiol. Biotechnol. 90 (2011) 1847–1868.
[8] C. Pulgarin, J. Kiwi, V. Nadtochenko, Appl. Catal. B-Environ. 128 (2012) 179–183.
[9] S. Rtimi, S. Giannakis, M. Bensimon, C. Pulgarin, R. Sanjines, J. Kiwi, Appl. Catal. B: Environ. 191 (2016) 42–52.
[10] S. Rtimi, S. Giannakis, R. Sanjines, C. Pulgarin, M. Bensimon, J. Kiwi, Appl. Catal. B: Environ. 182 (2016) 277–285.
[11] A. Bozzi, T. Yuranova, J. Kiwi, J. Photochem. Photobiol. A 172 (2005) 27–34.
[12] P.J. Kelly, R.D. Arnell, Vacuum 56 (2000) 159–172.
[13] S. Rtimi, R. Sanjines, M. Andrzejczuk, C. Pulgarin, A. Kulik, J. Kiwi, Surf. Coat. Technol. 254 (2014) 333–343.
[14] L. Brook, P. Evans, H. Foster, M. Pemble, A. Steele, D. Sheel, H. Yates, J. Photochem. Photobiol. A: Chem. 187 (2007) 53–63.
[15] L. Suárez, C. Pulgarin, C. Roussel, J. Kiwi, Appl. Catal. A Gen. 516 (2016) 70–80.
[16] L. Suárez, O. Baghriche, S. Rtimi, C. Pulgarin, J. Kiwi, J. Photochem. Photobiol. A: Chem. 330 (2016) 163–168.
[17] T.-D. Pham, B.-K. Lee, Appl. Surf. Sci. 296 (2014) 15–23.
[18] A.A. Alswat, M.B. Ahmad, M.Z. Hussein, N.A. Ibrahim, T.A. Saleh, J. Mater. Sci. Technol. 33 (2017) 889–896.
[19] C. Ruales-Lonfat, J.F. Barona, A. Sienkiewicz, M. Bensimon, J. Vélez-Colmenares, N. Benítez, C. Pulgarín, Appl. Catal. B: Environ. 166–167 (2015) 497–508.
[20] S. Giannakis, S. Liu, A. Carratalà, S. Rtimi, M.T. Amiri, M. Bensimon, C. Pulgarin, J. Hazard. Mater. 339 (2017) 223–231.
[21] J.I. Nieto-Juarez, T. Kohn, Photochem. Photobiol. Sci. 12 (2013) 1596–1605.
[22] C. Pulgarin, P. Peringer, P. Albers, J. Kiwi, J. Mol. Catal. A-Chem. 95 (1995) 61–74.
[23] H.Y. Xu, M. Prasad, Y. Liu, J. Hazard. Mater. 165 (2009) 1186–1192.
[24] S. Parra, L. Henao, E. Mielczarski, J. Mielczarski, P. Albers, E. Suvorova, J. Guindet, J. Kiwi, Langmuir 20 (2004) 5621–5629.
[25] Y.C. Li, L.G. Bachas, D. Bhattacharyya, Ind. Eng. Chem. Res. 46 (2007) 7984–7992.
[26] J.H. Ramirez, F.J. Maldonado-Hodar, A.F. Perez-Cadenas, C. Moreno-Castilla, C.A. Costa, L.M. Madeira, Appl. Catal. B-Environ. 75 (2007) 312–323.
[27] X.H. Liu, R. Tang, Q. He, X.P. Liao, B. Shi, Ind. Eng. Chem. Res. 48 (2009) 1458–1463.
[28] F. Mazille, A. Moncayo-Lasso, D. Spuhler, A. Serra, J. Peral, N.L. Benítez, C. Pulgarin, Chem. Eng. J. 160 (2010) 176–184.
[29] L. Suárez, H. Dong, C. Pulgarin, R. Sanjines, Z. Qiang, J. Kiwi, Appl. Catal. A Gen. 519 (2016) 68–77.
[30] B. Jansen, W. Kohnen, J. Ind. Microbiol. 15 (1995) 391–396.
[31] S. Rtimi, C. Pulgarin, R. Sanjines, J. Kiwi, RSC Adv. 5 (2015) 80203–80211.
[32] M. Kosmulski, E. Maczka, E. Jartych, J.B. Rosenholm, Adv. Colloid Interface Sci.

103 (2003) 57–76.
[33] C.M. Chan, T.M. Ko, H. Hiraoka, Surf. Sci. Rep. 24 (1996) 1–54.
[34] P. Villegas- Guzman, S. Giannakis, S. Rtimi, D. Grandjean, M. Bensimon, L.F. de Alencastro, R. Torres-Palma, C. Pulgarin, Appl. Catal. B 219 (2017) 538–549.
[35] S. Giannakis, A.I. Merino Gamo, E. Darakas, A. Escalas-Cañellas, C. Pulgarin, Solar Energy 98 (Part C) (2013) 572–581.
[36] M. Mangayayam, J. Kiwi, S. Giannakis, C. Pulgarin, I. Zivkovic, A. Magrez, S. Rtimi, Appl. Catal. B: Environ. 202 (2017) 438–445.
[37] F. Achouri, M. BenSaid, L. Bousselmi, S. Corbel, R. Schneider, A. Ghrabi, Environ Sci Pollut Res (2018) 1–10.
[38] D.Y. Goswami, D.M. Trivedi, S.S. Block, J. Sol. Energy Eng. 119 (1997) 92–96.
[39] C. Guillard, T.-H. Bui, C. Felix, V. Moules, B. Lina, P. Lejeune, Comptes Rendus Chim. 11 (2008) 107–113.
[40] N. Ogata, M. Sakasegawa, T. Miura, T. Shibata, Y. Takigawa, K. Taura, K. Taguchi, K. Matsubara, K. Nakahara, D. Kato, K. Sogawa, H. Oka, Pharmacology 97 (2016) 301–306.
[41] A. Pal, S.O. Pehkonen, L.E. Yu, M.B. Ray, J. Photochem. Photobiol. A: Chem. 186 (2007) 335–341.
[42] M. Vijay, K. Ramachandran, P.V. Ananthapadmanabhan, B. Nalini, B.C. Pillai, F. Bondioli, A. Manivannan, R.T. Narendhirakannan, Curr. Appl. Phys. 13 (2013) 510–516.
[43] A. Vohra, D.Y. Goswami, D.A. Deshpande, S.S. Block, Appl. Catal. B: Environ. 64 (2006) 57–65.
[44] C.D. Wanger, W.M. Riggs, L.E. Davis, J.F. Moulder, G.E. Muilenberg, Handbook of X-ray Photoelectron Spectroscopy Perkin-Elmer Corp., Physical Electronics Division, Eden Prairie, Minnesota, USA, 1979. Heyden & Son Ltd., 1979.
[45] J. Nogier, M. Delamar, P. Ruiz, B. Delmon, J.P. Bonnelle, M. Guelton, L. Gengembre, J.C. Vedrine, M. Brun, P. Albers, K. Seibold, M. Baerns, H. Papp, J. Stoch, L.T. Andersson, J. Kiwi, R. Thampi, M. Gratzel, G.C. Bond, N. Verma, J.C. Vickerman, R.H. West, Catal. Today 20 (1994) 109–123.
[46] D.A. Shirley, Phys. Rev. B 5 (1972) 4709–4714.
[47] E. Matijevic, P. Scheiner, J. Colloid Interface Sci. 63 (1978) 509–524.
[48] R.M. Cornell, U. Schwertmann, The Iron Oxides: Structure, Properties, Reactions, Occurrences and Uses, John Wiley & Sons, 2003.
[49] A. Groysman, Corrosion for Everybody, Springer, Netherlands, 2009.
[50] Y. Zheng, Z. Zhang, C. Li, J. Mol. Catal. A: Chem. 423 (2016) 463–471.
[51] W. Stumm, G.F. Lee, Ind. Eng. Chem. 53 (1961) 143–146.
[52] B. Movchan, A. Demchishin, Fiz. Metal. Metalloved. 28 (Oct 1969) (1969) 653–660.
[53] I. Petrov, P. Barna, L. Hultman, J. Greene, J. Vac. Sci. Technol. A: Vac. Surf. Films 21 (2003) S117–S128.
[54] S. Rtimi, C. Pulgarin, V.A. Nadtochenko, F.E. Gostev, I.V. Shelaev, J. Kiwi, Sci. Rep. 6 (2016) 30113.
[55] J. Marugan, R. van Grieken, C. Sordo, C. Cruz, Appl. Catal. B-Environ. 82 (2008) 27–36.
[56] J.V. Barth, G. Costantini, K. Kern, Nature 437 (2005) 671–679.
[57] L.F. González-Bahamón, F. Mazille, L.N. Benítez, C. Pulgarín, J. Photochem. Photobiol. A: Chem. 217 (2011) 201–206.